5.3 A simple model for the live fuel moisture of chamise

Robert G. Fovell *

Department of Atmospheric and Oceanic Sciences, University of California, Los Angeles

Tom Rolinski

U.S. Forest Service, Pacific Southwest Region, Fire and Aviation Management, Operations Southern California

Yang Cao

Department of Atmospheric and Oceanic Sciences, University of California, Los Angeles

ABSTRACT

Plant moisture content plays an important role in determining the availability of natural fuels for wildfires in Mediterranean ecosystems. While dead fuel moisture variation mainly depends exclusively on the weather conditions, live fuel moisture content is relatively more difficult to predict due to its seasonality in response to the physiological and phenological processes of plants such as spring flushing and fall curing as well as soil water availability. Efforts have been made using some kind of indices that employ routinely measured meteorological parameters to model live plant moisture content, such as the Keetch-Byram drought index (Keetch and Byram 1968), the cumulative water balance index (Dennison et al. 2003), field-sampled soil moisture (Qi et al. 2012), among others.

Our study aims to develop a simple, yet skillful model to predict live fuel moisture content of *Adenostoma fasciculatum* (chamise or greasewood) as measured at ten southern California sites. Data collected at these locations is used to help determine the kind of fire behavior (i.e. spread rate, intensity, etc.) that could be associated with wildfires across southern California. The key variable is soil moisture from the 40-100 cm layer derived from the North American Land Data Assimilation System (NLDAS) reanalysis. Our model consists of a time function to represent the average annual cycle and soil moisture differences from its own annual variation to capture LFM departures from normal. With this approach, correlation coefficients for the most accurately modeled sites exceed 0.8, if a time lag of 29 days is incorporated. As we are employing a gridded reanalysis, our strategy facilitates the reconstruction of past events as well as data gap filling. The improved live fuel moisture model can work with other components of fuel moisture to help monitor vegetation conditions in southern California regions for fire danger assessment.

1. Introduction

Live fuel moisture (LFM) is a measure of the moisture content of vegetation, which is important owing to its recognized role in the fire hazard (Pyne et al. 1996; Schoenberg et al. 2003). Large fires often occur during periods of low LFM (Dennison and Moritz 2009), with size increasing as LFM decreases (Davis and Michaelsen 1995). LFM is the ratio of the water weight in a particular sample to its dry weight, expressed as a percentage (Pollet and Brown 2007). Owing to its formulation, the LFM can exceed 100%, and often does during wet conditions.

While a variety of vegetation species are routinely sampled, the primary emphasis in southern California is on chamise or greasewood (*Adenostoma fasciculatum*), a common shrub that grows in the chaparral and is particularly flammable due to its fine, needle-like leaves and other characteristics (Countryman and Philpot 1970). Fuel moisture samples are usually taken twice a month by various fire agencies across southern California, using the technique described in Countryman and Dean (1979); see also Zahn and Henson (2011). Unfortunately, the sampling sites are sparse and the sampling times are not coordinated between fire agencies. In addition, the equipment used to dry the samples is not standardized which can lead to inconsistencies in the data. The fact that the age of the sampled material may vary from site to site is another complicating factor, as when moisture is abundant, new growth can contain much more water than older parts of the plant. It is understood that limited sample size implies a sizable amount of uncertainty in LFM measurements (Weise et al. 1998).

Over the years, there have been a number of attempts to model LFM for various species, especially employing easily obtained or computed meteorological information (e.g., Viegas et al. 2001; López et al. 2002; Castro et al. 2003), although it is recognized that such information alone

cannot fully describe the moisture content of live vegetation (Fiorucci et al. 2007). Dennison et al. (2003) evaluated the skill of models based on the Keetch-Byram Drought Index (KBDI; Keetch and Byram 1968) and the Cumulative Water Balance Index (CWBI; Dennison et al. 2003), as well as remotely sensed data, in reproducing LFM values sampled at sites in the Santa Monica mountains. A skillful relationship between CWBI and LFM for several species, including chamise, was demonstrated. Qi et al. (2012) used soil moisture sampled in the field along with remotely sensed data to model LFM values measured from species of oak and sagebrush. Although mean absolute errors were still sizable (±20% of LFM), soil moisture measured in situ emerged as the most useful LFM proxy.

The recognized dependence of chamise LFM on soil moisture availability (Dennison et al. 2003) suggests that soil moisture could serve as a reasonable proxy for this species as well. However, sampling LFM is already labor-intensive and expanding the program to measure soil conditions at the same sites [as was done by Sternberg et al. (1996) and Qi et al. (2012), for example] would add to that burden. Regarding chamise, Dennison and Moritz (2009) demonstrated the utility of using rainfall that, after all, is the source of soil moisture. We elected to pursue a different strategy, and test whether a *readily available, gridded soil moisture product could be used to reproduce historical LFM values.* If completely successful, the resulting product would be of significant use in operational fire behavior forecasting, as the proxy could be applied to the enormous areas for which LFM sampling is unavailable. It would also be available to fill in temporal gaps in the observational record, as well as extend the historical record backward in time.

2. Data sources

Historical live fuel moisture data was obtained from the National Fuel Moisture Database (NFMD) website[1], supplemented by other sources. For this study, we are focusing on LFM sampling sites located in the mountains located north and west of the city of Los Angeles, encompassing parts of Los Angeles, Ventura and Santa Barbara counties, at which chamise samples have been taken. Most of the sites are located on south-facing mountain slopes (Fig. 1a), at elevations ranging from about 400 to 1200 m above mean sea level (Table 1). Only sites established prior to January 2006, indicated by the filled black circles, were considered (see Table 1 for site information), as these have sufficient observations available to characterize the annual LFM cycle, an important part of our analysis strategy. (Other stations exist, and those established between 2006 and 2009 are marked by the unfilled black circles.)

[1]http://www.wfas.net/nfmd/public/states_map.php?state=CA

In the subset of sites where both new and old growth chamise is reported, consisting of San Marcos, Reyes Creek and Rose Valley (SAN, REY and ROS on Fig. 1a), the new growth data are used. The starting date for the analyses varies among the stations (Table 1), for most being the first available observation after 1 January 2001. Owing to the smaller number of samples available, all data on hand for SAN, REY, and ROS were utilized. Each analysis ends with the last LFM sample prior to 30 June 2013, with the year following that period (to 15 April 2015) reserved for out-of-sample testing.

The North American Land Data Assimilation System (Mitchell et al. 2004; Xia et al. 2012a,b), Phase 2 (hereafter "NLDAS") reanalysis product was selected as the soil moisture data source. The NLDAS project combines available observations and model output to provide surface and subsurface information over the conterminous United States at $1/8^{th}$ degree spatial resolution. The NLDAS model employs several land surface models (LSMs), including the Noah model that is used in the operational weather forecasting models from the National Centers for Environmental Prediction (NCEP) and is also a popular choice of Weather Research and Forecasting (WRF; Skamarock et al. 2008) model users. While other available versions of the NLDAS dataset have been considered for this work, we will confine our present analyses to the Noah product.

A few stations have been intentionally excluded from this analysis. The Bouquet Canyon (BOU on Fig. 1a) record has several long gaps, including after the site was burned in the October 2007 wildfires. Upper Oso (OSO) is one of the more infrequently sampled locations, and has several long stretches of missing data. This site is located very near San Marcos (SAN) although on the other side of the narrow coastal range; the relatively coarse NLDAS grid cannot differentiate between the two anyway. Templin Highway (not shown on Fig. 1a) was established in 1990, and samples are being taken there at present, but data are missing for the years 1997 through 2012.

Subsequent to December 2011, a change in NLDAS data sources and interpolation strategy (Youlong Xia, personal communication) caused contamination of soil moisture information near the coastline. This affects three stations, Clark Motorway (CLA), Trippet Ranch (TRP) and Schueren Road (SCH), all in the Santa Monica mountains near Malibu and whose LFM samples tend to be highly correlated. For SCH, which was retained in this analysis, soil moisture from an unimpacted location one grid cell to the north is used instead; this has a small negative impact on model skill. This effectively shifts the station well inland, on the north side of the tall but narrow Santa Monica mountains, which the NLDAS can barely detect (Fig. 1a).

Chamise has a dual root system, "a broad, near-

surface system to take advantage of light winter storms and a deep root system to tap deeper sources of water during summer drought" (Henson et al. 1996) that can reach depths as large as 8 m (Lambers et al. 2008). Chamise's roots can penetrate down to weathered bedrock and exploit tiny cracks in unweathered bedrock, where deep water reservoirs are available, especially during the annual summer drought (Hellmers et al. 1955; Sternberg et al. 1996). The soil-bedrock boundary was found to be at a depth of 20-40 cm at an experimental site (1150 m elevation) in the foothills of the San Jacinto Mountains in southern California (Sternberg et al. 1996). The Noah LSM uses four soil layers, representing 0-10, 10-40, 40-100, and 100-200 cm below ground level, and it is not precisely clear which of these best represents the shrub's root zone. We tested several layers and layer combinations before settling on the 40-100 cm layer soil moisture (hereafter referred to as "SM") for this analysis.

Both LFM and SM data can be noisy, subject to sharp, but often short-lived spikes following precipitation events. In the case of LFM, the noisiness is exacerbated by the relatively infrequent sampling. Our emphasis is on capturing the somewhat longer temporal variations of fuel moisture that might better characterize the seasonal fire hazard, rather than short-lived undulations in the LFM record. Thus, we view short-term variations in both series as distractions.

In this regard, the Noah 40-100 cm layer has some practical advantages. Unlike the shallower layers near the surface, the moisture in this soil layer is less subject to the high frequency pulses that immediately follow precipitation events. The temporal variation at this level is still sizable, but the time needed for moisture to pass through the top two layers acts as a natural filter. In contrast, the depth and thickness of the lowest level, 100-200 cm, renders variation in that layer to be small. This is illustrated for a single site, Laurel Canyon (LAU on Fig. 1a), in Fig. 2a. Note only the more sizable and prolonged rainfall events propagate down to the lower two soil levels. Remaining short-period variations in the 40-100 cm record are removed with smoothing, via application of a $\pm$ 30 day unweighted filter (see red curve on Fig. 2a).

Our immediate goal is to create the simplest possible model that skillfully captures the temporal variation of LFM. Given the dual-root structure of chamise, a combination of both shallower and deeper soil moisture might represent an improvement over the approach outlined below. However, an inadvertent characteristic of the centered temporal filter is that it spreads a signal forward and backward in time. With a layered, gravity-driven soil moisture model, that is tantamount to expanding the depth of the root zone somewhat.

3. Analysis strategy

The goal of this study is to forge simple yet skillful models for predicting LFM using the gridded NLDAS soil moisture product. We will soon see that, at first glance, LFM and SM are not particularly well related, as each has its own, somewhat different, annual cycle. *It is hypothesized, however, that LFM departures from its annual cycle may be predictable with soil moisture deviations from its own seasonal variation.* Therefore, for each sampling site considered, annual cycle models will be constructed for both LFM and SM, and residuals from these models will be used in the prediction model.

a. LFM annual cycle

In general, LFM is influenced by a variety of factors, including moisture availability, evapotranspiration, and plant physiology (Qi et al. 2012). In the study area, nearly all of a typical year's precipitation falls in the non-summer months, so LFM values typically reach their lowest values in the fall, before the seasonal rains have commenced as is typical for a Mediterranean climate (McCutchan 1977; Moreno and Oechel 1994). For chamise, another control has to be air temperature, which to a certain extent, determines whether the shrub is active or dormant[2]. Due to dormancy, the vegetation at higher, cooler elevations may not take up moisture from the soil, even long after the winter rains have begun. The consequence of this is that the LFM of chamise has a pronounced annual cycle reflecting not only the temporal variation of rainfall, but also the influence of elevation.

This dependence can be seen in Fig. 2b, which shows the temporal variation of LFM for three stations over a five-year period. The vegetation at the intermediate elevation station, San Marcos (816 m), is the wettest of the group, likely reflecting its coastal location above Santa Barbara (Fig. 1a). Although this station's peak values vary substantially through the period, they tend to occur in the spring season, between March and May. In contrast, the lower (Laurel Canyon, 398 m) and higher (Reyes Creek, 1233 m) sites evinced earlier and later peaks, respectively, in three of the five years depicted.

The annual model for LFM will consist of a "time function" (TF) with an intercept and four additional terms, two sine and two cosine functions representing periods of 12 and 6 months (365.25 and 182.625 days), a combination is capable of identifying fairly oddly shaped annual cycles[3]. Two alternate strategies were pursued,

[2]The time of year when chamise begins to emerge from dormancy is dependent on temperature; however, after the reproduction cycle is over, the plant will begin to enter dormancy regardless of temperature.

[3]While statistically significant for most stations, the 6-month sine and cosine terms contribute only trivially to the time function, and could be excluded with relatively little loss of skill. However, this

with the regression applied to the original, irregularly spaced LFM dataset, and one that was interpolated to daily frequency using cubic splines. The latter approach is functionally a periodogram spectral analysis on equally-spaced data with the coefficients determined by linear regression. As anticipated, the two approaches yield nearly identical results for sufficiently long series without serious data gaps, and this is one reason why we restricted our analysis to more established and continually-sampled sites. It is important to note that a log transform is always applied to LFM data, as this helps to compress this positive definite and open-ended series, but LFM observations, reconstructions and residuals will be shown only after transformation back to the original units.

Figure 3a presents the LFM annual models for the ten stations selected for analysis, based on a day-of-year (DOY) measure that for convenience starts on September 1^{st}. This convention coincides with the climatological onset of the "Santa Ana" winds (Raphael 2003; Jones et al. 2010), the offshore flow that greatly increases the fire danger in southern California. It is clear that the annual cycles vary among the sites with respect to amplitude and phase. As was suggested by Fig. 2b, lower elevation stations tended to reach peak LFM earliest in the season. Laurel Canyon's peak is on DOY 214 (April 2^{nd} for a non-leap year). Reyes Creek, the highest elevation site sampled, has a long, slow increase through the wet season, peaking at DOY 261 (May 19^{th}). The anticipated dependence on peak DOY with elevation is imperfect but strong (Fig. 4). These LFM annual models account for between 45 to 74% of the original live fuel moisture variance (see R^2 values in Table 2). The best fit was for Schueren Road, which is very close to the coast, and the poorest was for the highest elevation station, Reyes Creek, which is also located far inland (Fig. 1a).

b. Soil moisture annual cycle

The long-term average and standard deviation of the 40-100 cm layer soil moisture in the NLDAS Noah-based reanalysis is shown in Fig. 1b. The temporal variation is small in the urbanized area, including nearby LFM sites Laurel Canyon, La Tuna Canyon (LAT on Fig. 1a) and Placerita Canyon (PLA). Glendora Ridge (GLE) and Peach Motorway (PEA) are located near pronounced local maxima and minima of soil moisture, respectively. The relatively coarse resolution of the NLDAS dataset is obvious, especially along the coastline. It is also apparent in a comparison of actual and interpolated station elevations (Table 2).

The time function approach was also applied to SM data, which NLDAS can provide on a daily basis. As with LFM, SM annual cycles were constructed using log-transformed values to suppress the natural increase of variability with magnitude. SM has a rather different annual cycle than LFM (Fig. 3b), generally being smoother in time and peaking earlier in the wet season. The soil moisture TFs capture between 46 and 71% of the original temporal variability (Table 2), comparable to the LFM annual models, and is highest at Rose Valley and lowest at Peach and Bitter Canyon (BIT on Fig. 1a).

With respect to phase and amplitude, the ten locations separate into two very distinct clusters, determined in part by soil characteristics such as texture (Fig. 1c), hydraulic conductivity, and field capacity. The three sites at the urban margin, Laurel Canyon, La Tuna Canyon and Placerita Canyon, share a relatively small amplitude variation with an early peak at DOY 172 (February 19^{th}) (Fig. 3b). The remaining stations reach peak soil moisture within a few days of DOY 194 (March 13^{th}). Most of the stations share the same annual mean, with San Marcos, Peach Motorway and Bitter Canyon emerging as different.

4. The modeling strategy, applied to Laurel Canyon

Our strategy is to predict the temporal changes of LFM using a time function in combination with SM. Specifically, we are concerned with SM's skill in capturing departures from a site's annual LFM cycle. After all, if a site deviates little from its established annual cycle, then climatology provides the best forecast. As already shown in Fig. 3a, climatology varies from station to station based on location, including elevation and, therefore, each station has a unique TF. It is emphasized that while interpolated LFM data are needed for model refinement, as shown below, the final LFM prediction models for each site were built using available LFM observations alone.

This strategy is applied to the Laurel Canyon site in Fig. 5. Observed LFM (black dots) is compared to the time function (red curve) for the period extending roughly from February 2001 through June 2013 (Fig. 5a). The TF captures a sizable 57% of the observed series' variance, which is the average for the 10 stations examined (Table 2). Removal of the clearly anomalous year of 2007 would increase the R^2 to 0.7, but without altering the annual cycle shape, or the findings that follow, very much. As a consequence, this year is retained for this and other locations.

The residuals from this fit (Fig. 5b) reveal a number of discrepancies of variable length and magnitude, some of which are important but may be difficult to discern prior to removal of the annual cycle. During the spring of 2002 (episode #1 on the figure), observed LFM values declined more rapidly than predicted by the time function, resulting in a several-month period of overprediction. The following

shorter period function helps refine the shape of the annual cycle the most at locations like Reyes Creek. We want to use equations with the same functional form at all stations.

year, LFM both increased more quickly during fall and waned more slowly in the spring (episode #2), creating an extended period with positive residuals. Episodes #3 and #5 involved temporally narrow spikes in LFM that occurred during otherwise more "normal" years, and episode #4 involved an early increase followed by a more typical decline towards low warm-season readings.

LFM values at this station remained very low during the profound drought of 2007 (episode #6). During this period, LFM values remained well below Dennison and Moritz (2009)'s critical threshold value of roughly 79%, under which fire sizes could be significantly larger. The years 2008-11 were characterized by slightly wetter than normal fuel moistures, culminating in a more rapid than usual increase in early 2011 (episode #7). The LFM rise was delayed in the winter of 2011, and the decline occurred earlier in the following year, representing the combined period marked episode #8.

The annual cycle for SM also captures 57% of its total variance (Fig. 5c), again roughly average for our ten stations (Table 2). Residuals from this fit (Fig. 5d) bear significant resemblance to the LFM annual model's departures, and direct comparison is facilitated by superimposing the two error series (Figs. 6a, d). This comparison illustrates the partial correlation between the LFM and SM series, adjusted for the time function, which can be written as r(LFM, SM | TF). The partial correlation may be computed by separately regressing LFM and SM on the time function and then correlating the resulting residuals (r_L and r_S), as done here. The resulting squared correlation is 0.55 ($r = 0.74$), which represents an appreciable contribution of skill to the LFM prediction model beyond what the TF itself could provide.

While the congruence between the error series is substantial, it is also readily apparent there is a *systematic phase difference* between them. Figs. 6b and e present the same data, after shifting the SM residuals later by 29 days[4]. This is tantamount to relating LFM today to SM anomalies from about a month prior, so that SM is a leading indicator of LFM or, equivalently, LFM lags SM. This makes the time interval between precipitation and the LFM response even longer, as it takes time for water received at the surface to percolate downward to the 40-100 cm layer (Fig. 2a). This result further suggests that chamise LFM is responding most directly and powerfully to SM changes farther below the surface, where the shrub's deeper taproots might be expected to reside.

After shifting the SM residual series, there is now a closer correspondence between these TF departures in terms of timing, and the squared partial correlation has increased to 0.66 ($r = 0.81$). The faster-than-expected decline of fuel moisture during the spring of 2002 (marked episode #1) corresponded with a more rapid than usual drop in SM, which had reached its own peak about 29 days earlier. LFM episodes #2-5 have significant, if imperfect, correspondences to SM variations, and episode #6 is dramatic in both series. (Naturally, the formal relationship between these series – the slope – will be determined by regression.) Even the small, higher frequency spikes during episodes #7 and 8 appear in the SM residuals.

The prediction model for Laurel Canyon LFM is given by

$$\begin{aligned}\log(LFM) &= intercept \ + \ TF + \ \log(SM) \\ &= \alpha \ + \ \beta_1 \cos(2\pi D/L) \ + \ \beta_2 \sin(2\pi D/L) \\ &+ \beta_3 \cos(4\pi D/L) \ + \ \beta_4 \sin(4\pi D/L) \ + \\ &\beta_5 \log(SM) \ + \epsilon,\end{aligned} \tag{1}$$

where α is the intercept, β_i are the slope coefficients, SM_{29} is soil moisture lagged by 29 days, D is September-based DOY, L is the length of year in days, and ϵ is the error. Predictions from this model, after removal of the log transform, are shown along with observations in Fig. 7, with the climatological TF also displayed for reference. Overall, the prediction model is quite skillful relative to climatology (R^2=0.85 vs. 0.57). The rapid decline of LFM during episode #1 is very well captured, as are episode #4's early increase, #2's delayed decline, and, especially, the dramatic drought of 2007 (episode #6). The sharp LFM peak during episode #3 is significantly underpredicted but the autumnal increase and springtime decline are well captured. The model does better with period #5's sharp peak, and the episodes marked #7 and 8 are also rather well handled.

Scatterplots of predicted vs. observed values can exaggerate the lack of fit (due to missing dimensions, such as frequency and time) but are useful for checking for heteroscedasticity. Results of the White (1980) test indicated heteroscedasticity is not a concern, which is due to the use of log transformations. The suggestion of nonconstant variance in Fig. 8 only appears after the log transformation is removed (not shown).

5. Other sites

Figure 9 presents prediction models for the ten stations in the study area. For each location, the model was trained using observations prior to 30 June 2013 (see Table 1), and also applied to the final, approximately two-year period (ending 15 April 2015) that was reserved for out-of-sample testing. While the figure and Table 2 reveal that our present SM and TF-based strategy worked best for Laurel Canyon, other stations with model $R^2 \geq 0.80$ include La Tuna Canyon, Schueren Road and San Marcos (Figs. 9c,

[4]The reason why 29 days lag is selected will be explained in Section 6.

g and h). Model performance during the out-of-sample period generally appears acceptable.

The goal of our LFM modeling is to gain skill on climatology, as represented by the LFM annual model. The average skill gain (see Table 2 and Fig. 10) by the full prediction model over the annual (TF) model was about 18%, and ranged from 28% (at Laurel Canyon) to 11% (at Schueren Road and Peach Motorway). The small skill gain at Schueren Road (Fig. 9g) reflects the fact that the LFM TF had already claimed a large 74% of the total variance, the largest percentage among all stations examined. LFM tends to vary little from year to year at this coastal location, even during drought years, relative to sites farther inland. The situation at Peach Motorway will be considered presently.

The poorest fit was found for one of the most inland locations, Reyes Creek (Fig. 9j). Lack of fit can result from a variety of reasons, including but not limited to improperly resolved topography, limitations associated with the precipitation estimation, inadequacies in the soil model, and local site characteristics, including drainage. In the case of Reyes Creek, the quality of the LFM annual model may be impacted by the less frequent sampling at that location. Overall, however, we believe the skillfulness of the fit at most stations is high enough to provide useful information for operations, particularly for the timing of LFM increases and decreases through the Dennison-Moritz critical fire weather threshold.

There is a strong similarity among these time series, because they all share a fundamentally similar annual cycle. However, it is worth examining more closely how LFM and the prediction models behaved during the 2007 drought. Figure 11 focuses in on this period, highlighting stations Laurel Canyon, Placerita Canyon and San Marcos. As previously seen, LFM at Laurel Canyon hardly changed at all during this period (Fig. 11a), resulting in very large anomalies relative to climatology. Plant moisture had fallen below the Dennison-Moritz threshold by August 2006, and never exceeded it again until after January 2008. This anomalous behavior is reproduced by the prediction model, and a similar phenomenon is also seen at Bitter Canyon and Reyes Creek (Figs. 9f, j).

At other locations, the 2007 drought was not quite as dramatic. At Placerita Canyon (Fig. 11b), for instance, LFM values rose above 80% for a short time during May 2007 before quickly falling again. As occurs at other sites, the Placerita prediction equation handles some periods of declining LFM better than others, so some additional model refinement is clearly possible. At coastal sites San Marcos (Fig. 11c) and Schueren Road (Fig. 9g) the year of 2007 did not appear particularly unusual at all as their soil moistures were able to recover during the nominal wet season, consistent with their relatively higher fuel moisture readings. Taken together, these results indicate that spatial variations in LFM during the drought were associated with subtle differences in local soil moisture conditions that were faithfully captured in the NLDAS reanalysis and, therefore, the SM-based LFM prediction models.

The prediction models clearly have difficulty in capturing the largest values of LFM that can occur during the wet season, especially when LFM exceeds 100% or so. This is particularly true at stations Placerita Canyon and Glendora Ridge (Figs. 9b, i), for which the models consistently underpredict peak LFM values[5]. It is possible that a model based only on SM and climatology cannot realistically predict very large LFM values anyway, as they may represent situations in which the plant condition is not intrinsically limited by the available soil moisture. This is part of the increase of variation with LFM magnitude that the log transformations were employed to suppress. However, in practice, this is not an issue for us because the fire danger is lower when LFM values are large. We would sacrifice accuracy in predicting large peak values for model skill in capturing the temporal shifts between more and less dangerous plant moisture values.

6. Lag and location issues

For simplicity, all of the fits shown in Fig. 9 and Table 2 employed a 29-day lag with SM. This time interval proved optimal for Laurel Canyon, as seen in Fig. 12a, which presents the partial correlation between the residual series r_L and r_S. This plot was constructed from daily SM data along with cubic spline-interpolated LFM information. Especially owing to the smoothing applied to the SM data, the variation with lag is not very large, making the results somewhat less sensitive to the precise time interval employed.

The optimal lag, however, is found to vary among the sites, ranging from 0 days at Peach Motorway to 38 days at Glendora Ridge (Table 2). Figure 12b suggests there are three distinct behaviors relative to Laurel Canyon exhibited: Placerita Canyon, Glendora Ridge and La Tuna Canyon, located in the eastern part of the study area, tend to have longer lags between SM and LFM, and the correlation drops off quickly for negative lags (LFM leading SM); San Marcos and Rose Valley in the western part of the study area tend to have somewhat shorter lags; and Schueren Road and Bitter Canyon, located in between, had very short lags with a slow drop-off of correlation for negative values. The LFM-SM time lag also tended to increase with elevation, clearly separating into two distinct groupings (Fig. 13), separating out stations Laurel, Placerita, and La Tuna Canyons already seen as different with respect to soil moisture in Fig. 3b. (The reason

[5]The impact of this on the regressions is mitigated by the log transformations.

why Glendora Ridge also falls into the group is presently unknown.) Unfortunately, this complicates the effort to create a single prediction model applicable to all sites, which would be useful for operational reasons.

Note for positive lags (SM leading LFM), no station has a partial correlation higher than Laurel Canyon. As a consequence, perhaps this site should not determine the common network lag. That being said, we could certainly employ a different lag for each site, but in most cases the skill improvement is minor (as suggested by a comparison between maximum and lag 29 partial correlations in Table 2), with the possible exception of two locations: Peach Motorway and Bitter Canyon.

The extremely very short LFM-SM lags for Peach and Bitter emerge as anomalies, and may represent issues associated with the NLDAS reanalysis' coarse resolution and/or the representativeness of NLDAS soil conditions for those sites. On the NLDAS grid, Peach is located very near a locally dry area (Fig. 1b) representing the urbanized area of Santa Clarita, which is (likely inappropriately) impacting the SM at the Peach site. Bitter Canyon resides very close to a large reservoir, Castaic Lake, although that feature is not represented in the NLDAS land mask at all. Yet, using nearby Placerita Canyon's soil moisture information in the Peach and Bitter Canyon models results in improved fits (not shown) at both locations (R^2 = 0.82 vs. 0.74 at Peach, and R^2 = 0.76 vs. 0.70 at Bitter, labeled as "modified" in Table 2), with optimal lag times closer to the multi-site average. To a large degree, using Placerita SM means essentially adopting that site's soil characteristics in place of their NLDAS assignments.

It might be wondered how the Laurel Canyon fit would fare if soil moisture from another (termed "shifted") location were used in the prediction model. Figure 6c replaces the site's SM information with that from a grid point (see star in Fig. 1) located 44 km to the northwest, at the station's original altitude but in the region of soil texture class 6 (loam; Fig. 1c) that occupies a large (and relatively unsampled) portion of the study area. While the gross features representing the regional weather variations have not changed much, and the displacement is only 3-4 NLDAS grid points, the fit is clearly poorer (Fig. 6f), even at the (shorter, 12 day) lag that maximizes the partial correlation. Finally, it might also be wondered how *unsmoothed* soil moisture might fare in these prediction models. At every site, the use of unsmoothed SM information results in *diminished skill* (not shown), mainly because SM acquires high frequency spikes that do not match up well with the noisy LFM data. However, this creates more of an appearance than a reality of reduced skill.

7. Concluding discussion

In this study, we have outlined a viable and simple strategy for reconstructing the historical variation of chamise LFM and for making short-term LFM forecasts in the mountainous region northwest of Los Angeles on a site-by-site basis. The live fuel moisture of chamise is considered a very important indicator of the fire threat in Southern California. Currently, chamise LFM is sampled irregularly through the year at scattered locations in the area's mountains. Our strategy makes use of a readily available, gridded soil moisture (SM) product provided by the NLDAS, which enables us to fill in temporal gaps in the LFM record as well as reconstruct past events. For this study, we adopted the version of the NLDAS dataset that employed the Noah land surface model.

Specifically, the prediction model for each site consists of a time function and the moisture of the 40-100 cm soil layer. The latter is considered as indicative of the moisture available to the plants' roots. The time function reconstructs the LFM annual variation. Owing to the properties of regression analysis, we can consider the model as consisting of a correlation of LFM departures from climatology with deviations of SM from its own annual cycle.

An important characteristic of the model is that LFM deviations were found to lag SM variations from climatology. The lag was site-dependent, ranging between 12 and 38 days (neglecting sites with resolution-influenced representativeness issues), with an average close to one month although generally increasing with site elevation. Stations at higher elevations tended to have a later LFM peak time, as mean temperature decreases with altitude and higher sites are often associated with cloudier weather (i.e., less available sunshine). Additionally, soil texture, porosity, and other characteristics vary through the study area, influencing how rapidly precipitation reaches the root zone and also how quickly the soil subsequently dries out after the rains cease. Some difficulties that arose owing to the coarse resolution of the NLDAS dataset were discussed.

The LFM-SM lag has important practical implications for operational monitoring of live fuel moisture. The NLDAS is not available in real time, but is instead delayed by several days. The roughly one-month lag permits us time to not only obtain the needed soil data but also to apply some temporal filtering to smooth out some of the higher frequency information that is not currently considered useful. The lag also permits us to anticipate how LFM might be changing over the short term.

There are a number of avenues through which this analysis strategy could be improved. To keep the model simple, we explicitly considered only one of the four available soil layers in the Noah-based NLDAS dataset. A weighted combination of layers might be indicated,

especially for a plant with a complex root structure such as chamise. Other versions of the NLDAS utilize different land surface models, which utilize different assumptions leading to different information about SM availability. These versions might be combined in an ensemble sense to provide more accurate SM input to the prediction model. A higher resolution dataset would very likely assist with problems we encountered with coastal and also the highest elevation sampling sites.

The most useful practical improvement would be the development of a single equation that could predict LFM for all sites, given day of year and SM inputs. Such an equation would have to incorporate elevation effects seen in Figs. 3a and 4, and perhaps other meteorological information, such as marine layer influences that influence differences in plant behavior between coastal and inland sites. This is left for future work.

Acknowledgments.

This research was sponsored by the San Diego Gas & Electric Company. The authors thank David Weise for his constructive discussions and suggestions, and Travis Wilson for his ideas.

REFERENCES

Castro, F., A. Tudela, and M. Sebastià, 2003: Modeling moisture content in shrubs to predict fire risk in Catalonia (Spain). *Agricultural and Forest Meteorology*, **116 (1)**, 49–59, doi:10.1016/S0168-1923(02)00248-4.

Countryman, C. M. and W. A. Dean, 1979: *Measuring moisture content in living Chaparral: A field user's manual*. General Technical Report PSW-36, U.S. Department of Agriculture, Forest Service, Pacific Southwest Forest and Range Experiment Station, 27 pp., URL `http://www.treesearch.fs.fed.us/pubs/24092`.

Countryman, C. M. and C. W. Philpot, 1970: *Physical Characteristics of Chamise as a Wildland Fuel*. Research Paper PSW-66, U.S. Department of Agriculture, Forest Service, Pacific Southwest Forest and Range Experiment Station, 16 pp., URL `http://www.fs.fed.us/psw/publications/documents/psw_rp066/psw_rp066.pdf`.

Davis, F. W. and J. Michaelsen, 1995: Sensitivity of fire regime in chaparral ecosystems to climate change. *Global Change and Mediterranean-type Ecosystems*, J. M. Moreno and W. C. Oechel, Eds., Springer-Verlag, New York, NY, 435–456.

Dennison, P. E. and M. A. Moritz, 2009: Critical live fuel moisture in chaparral ecosystems: A threshold for fire activity and its relationship to antecedent precipitation. *Int. J. Wildland Fire*, **18 (8)**, 1021–1027, doi:10.1071/WF08055.

Dennison, P. E., D. A. Roberts, S. R. Thorgusen, J. C. Regelbrugge, D. Weise, and C. Lee, 2003: Modeling seasonal changes in live fuel moisture and equivalent water thickness using a cumulative water balance index. *Remote Sensing of Environment*, **88 (4)**, 442–452, doi:10.1016/j.rse.2003.08.015.

Fiorucci, P., F. Gaetani, A. Lanorte, and R. Lasaponara, 2007: Dynamic fire danger mapping from satellite imagery and meteorological forecast data. *Earth Interact.*, **11 (7)**, 1–17, doi:10.1175/EI199.1.

Hellmers, H., J. Horton, G. Juhren, and J. O'keefe, 1955: Root systems of some chaparral plants in Southern California. *Ecology*, **36 (4)**, 667–678, doi:10.2307/1931305.

Henson, P., D. Usner, and V. Kells, 1996: *The natural history of Big Sur*. California Natural History Guides, University of California Press.

Jones, C., F. Fujioka, and L. M. V. Carvalho, 2010: Forecast Skill of Synoptic Conditions Associated with Santa Ana Winds in Southern California. *Monthly Weather Review*, **138**, 4528–4541, doi:10.1175/2010MWR3406.1.

Keetch, J. and G. Byram, 1968: *A drought index for forest fire control*. Research Paper SE, U.S. Department of Agriculture, Forest Service, Southeastern Forest Experiment Station, 35 pp., URL `http://www.treesearch.fs.fed.us/pubs/40`.

Lambers, H., F. Chapin, and T. Pons, 2008: *Plant physiological ecology*. Springer-Verlag, New York, NY, 605 pp.

López, A. S., J. San-Miguel-Ayanz, and R. E. Burgan, 2002: Integration of satellite sensor data, fuel type maps and meteorological observations for evaluation of forest fire risk at the pan-European scale. *Int. J . Remote Sens.*, **23**, 2713–2719, doi:10.1080/01431160110107761.

McCutchan, M. H., 1977: Climatic features as a fire determinant. *Symposium on the Environmental Consequences of Fire and Fuel Management in Mediterranean Ecosystems. Palo Alto, CA*, H. A. Mooney and C. E. Conrad, Eds., U.S. Department of Agriculture, Forest Service, Washington Office,Washington, DC, General Technical Report WO-3, 1–11, URL `https://archive.org/details/CAT78696401`.

Mitchell, K. E., et al., 2004: The multi-institution North American Land Data Assimilation System (NLDAS): Utilizing multiple GCIP products and partners in a continental distributed hydrological modeling system. *J. Geophys. Res.-Atmos.*, **109**, D07S90, doi:10.1029/2003JD003823.

Moreno, J. M. and W. C. Oechel, 1994: The role of fire in mediterranean-type ecosystems. *Ecological studies (USA)*, doi:10.1007/978-1-4613-8395-6.

Pollet, J. and A. Brown, 2007: *Fuel moisture sampling guide*. U. S. Bureau of Land Management, Utah State Office, Salt Lake City, UT, 32 pp., URL `http://www.wfas.net/nfmd/references/fmg.pdf`.

Pyne, S., P. Andrews, and R. Laven, 1996: *Introduction to wildland fire, 2^{nd} edition*. Wiley-Interscience Publication, John Wiley & Sons, Ltd, 808 pp.

Qi, Y., P. E. Dennison, J. Spencer, and D. Riaño, 2012: Monitoring live fuel moisture using soil moisture and remote sensing proxies. *Fire Ecol.*, **8 (3)**, 71–87, doi:10.4996/fireecology.0803071.

Raphael, M., 2003: The Santa Ana winds of California. *Earth Interact.*, **7 (8)**, 1–13, doi:10.1175/1087-3562(2003)007⟨0001:TSAWOC⟩2.0.CO;2.

Schoenberg, F. P., R. Peng, Z. Huang, and P. Rundel, 2003: Detection of non-linearities in the dependence of burn area on fuel age and climatic variables. *Int. J. Wildland Fire*, **12 (1)**, 1–6, doi:10.1071/WF02053.

Skamarock, W. C., et al., 2008: A description of the Advanced Research WRF version 3. Tech. rep., NCAR Technical Note, 125 pp., Boulder, CO. URL `http://www2.mmm.ucar.edu/wrf/users/docs/arw_v3.pdf`.

Sternberg, P., M. Anderson, R. Graham, J. Beyers, and K. Tice, 1996: Root distribution and seasonal water status in weathered granitic bedrock under chaparral. *Geoderma*, **72 (1)**, 89–98, doi:10.1016/0016-7061(96)00019-5.

Viegas, D., J. Piñol, M. Viegas, and R. Ogaya, 2001: Estimating live fine fuels moisture content using meteorologically-based indices. *Int. J. Wildland Fire*, **10 (2)**, 223–240, doi:10.1071/WF01022.

Weise, D. R., R. A. Hartford, and L. Mahaffey, 1998: Assessing live fuel moisture for fire management applications. *Fire in ecosystem management: Shifting the paradigm from suppression to prescription*, T. L. Pruden and L. A. Brennan, Eds., Tall Timbers Research Station, Tallahassee, FL, Tall Timbers Fire Ecology Conference 20^{th} Proceedings, Vol. 20, 49–55, URL `http://www.fs.fed.us/psw/publications/4403/psw_1998_weise000.pdf`.

Xia, Y., et al., 2012a: Continental-scale water and energy flux analysis and validation for north american land data assimilation system project phase 2 (nldas-2): 2. validation of model-simulated streamflow. *J. Geophys. Res.-Atmos.*, **117 (D03110)**, doi:10.1029/2011JD016051.

Xia, Y., et al., 2012b: Continental-scale water and energy flux analysis and validation for the north american land data assimilation system project phase 2 (nldas-2): 1. intercomparison and application of model products. *J. Geophys. Res.-Atmos.*, **117 (D03109)**, doi:10.1029/2011JD016048.

Zahn, S. and C. Henson, 2011: *Fuel Moisture Collection Methods: A Field Guide*. 1151 1803P, USDA Forest Service San Dimas Technology and Development Center, 11 pp., URL `http://www.fs.fed.us/t-d/php/library_card.php?p_num=1151%201803P`.

TABLE 1. Live fuel moisture sites elevation and the R-squares of the models.

Abbreviation	Station	Elevation (m)	Time period	# LFM samples	Soil texture
LAU	Laurel Cyn	398	2/5/01-6/27/13	285	2 (loamy sand)
LAT	La Tuna Cyn	610	1/8/04-6/27/13	215	2 (loamy sand)
PLA	Placerita Cyn	602	1/8/01-6/27/13	288	3 (sandy loam)
PEA	Peach Motorway	579	1/22/05-6/27/13	217	2 (loamy sand)
PEA	Peach Motorway *modified*	579	1/22/05-6/27/13	217	6 (loam)
GLE	Glendora Ridge	751	11/12/02-6/27/13	227	6 (loam)
BIT	Bitter Cyn	532	1/8/01-6/27/13	291	6 (loam)
BIT	Bitter Cyn *modified*	532	1/8/01-6/27/13	291	9 (clay loam)
SCH	Schueren Rd	678	1/8/01-6/27/13	288	6 (loam)
SAN	San Marcos	816	4/1/00-6/27/13	176	6 (loam)
ROS	Rose Vly	1096	5/1/00-6/27/13	162	6 (loam)
REY	Reyes Ck	1233	1/15/04-6/27/13	145	2 (loamy sand)

TABLE 2. Live fuel moisture annual and prediction model information.

Abbreviation	Station	Elevation (m)	NLDAS elevation (m)	LFM annual model R^2	Soil moisture annual model R^2	Max partial correlation (lag)	Partial correlation at lag 29	Full model R^2
LAU	Laurel Cyn	398	100	0.57	0.57	0.81 (29)	0.81	0.85
LAT	La Tuna Cyn	610	324	0.61	0.54	0.69 (35)	0.68	0.82
PLA	Placerita Cyn	602	513	0.55	0.54	0.73 (36)	0.72	0.78
PEA	Peach Motorway	579	526	0.63	0.47	0.54 (0)	0.48	0.74
PEA	Peach Motorway *modified*	579	513	0.63	0.55	0.66 (21)	0.66	0.82
GLE	Glendora Ridge	751	636	0.59	0.57	0.67 (38)	0.67	0.77
BIT	Bitter Cyn	532	695	0.48	0.46	0.68 (3)	0.64	0.70
BIT	Bitter Cyn *modified*	532	513	0.48	0.54	0.74 (32)	0.74	0.76
SCH	Schueren Rd *shifted*	678	385	0.74	0.68	0.67 (12)	0.65	0.84
SAN	San Marcos	816	566	0.63	0.69	0.56 (19)	0.55	0.83
ROS	Rose Vly	1096	1295	0.55	0.71	0.59 (18)	0.59	0.70
REY	Reyes Ck	1233	1399	0.45	0.68	0.42 (28)	0.42	0.61

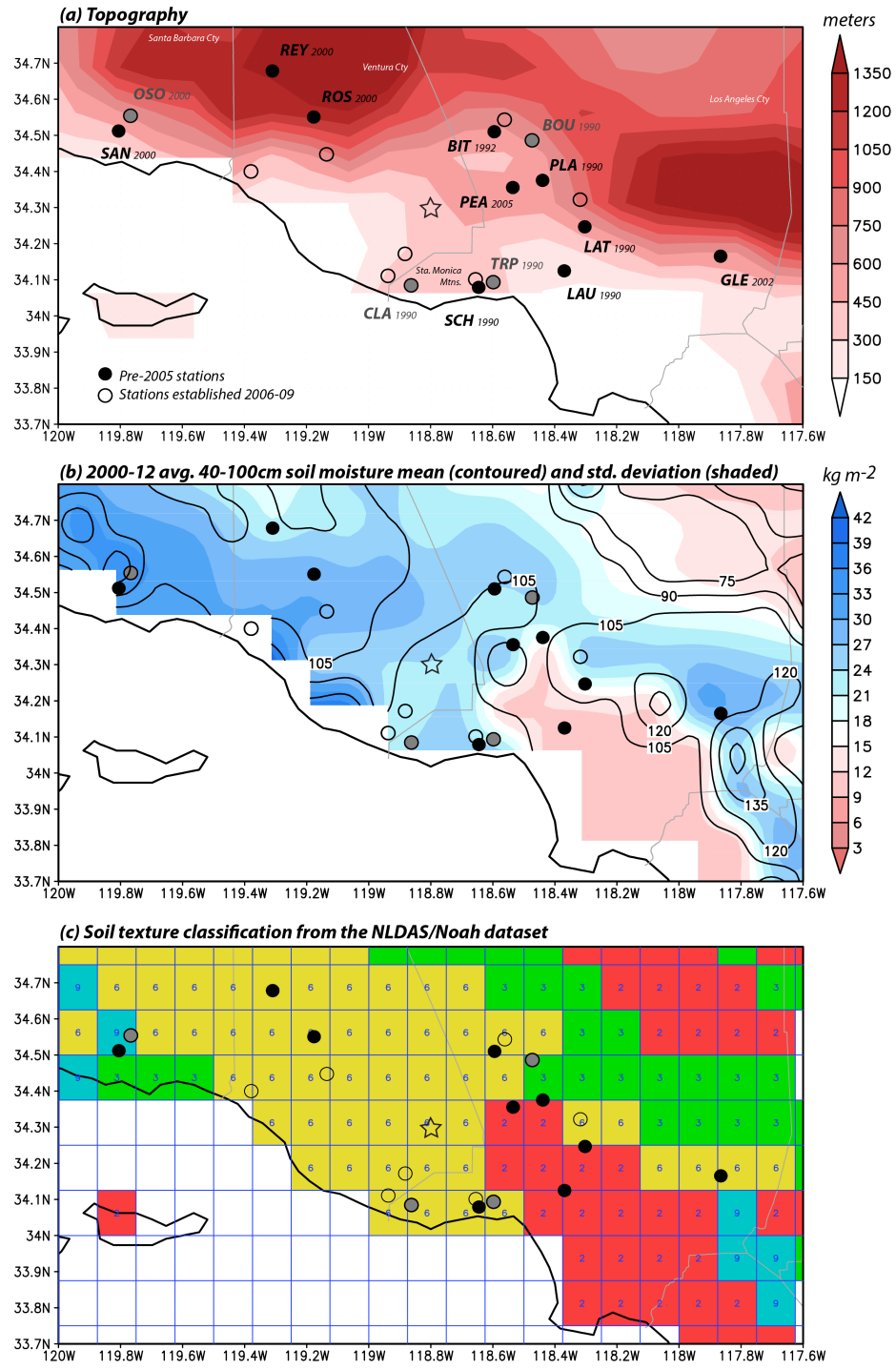

FIG. 1. (a) Live Fuel Moisture surface site locations (black dots), with underlying topography (meters) shaded, along with station abbreviations (see Table 1) and year site established; (b) 2000-2012 averaged 40-100cm layer soil moisture (kg m^2) mean (contoured) and standard deviation (shaded); and (c) Soil texture classification over Southern California, all from the NLDAS/Noah dataset. Texture classes shown include: 2 (loamy sand), 3 (sandy loam), 6 (loam) and 9 (clay loam). Excluded stations marked in grey. Star indicates "shifted" soil moisture location used in Laurel Canyon sensitivity test (see text).

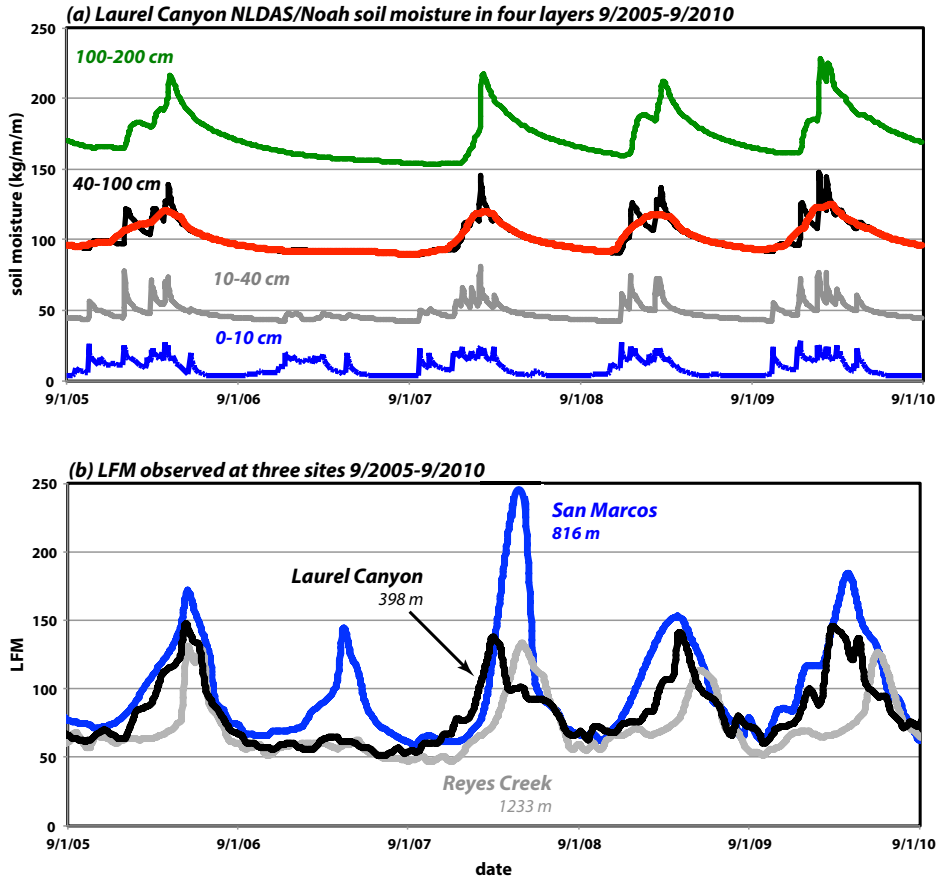

FIG. 2. (a) Laurel Canyon site soil moisture in four layers (0-10, 10-40, 40-100, and 100-200 cm) for September 2005-September 2010 from the NLDAS/Noah dataset; and (b) Observed LFM at Laurel Canyon, Reyes Creek and San Marcos September 2005-September 2010. The red curve in (a) represents 40-100 cm soil moisture smoothed with a $\pm$ 30 day filter.

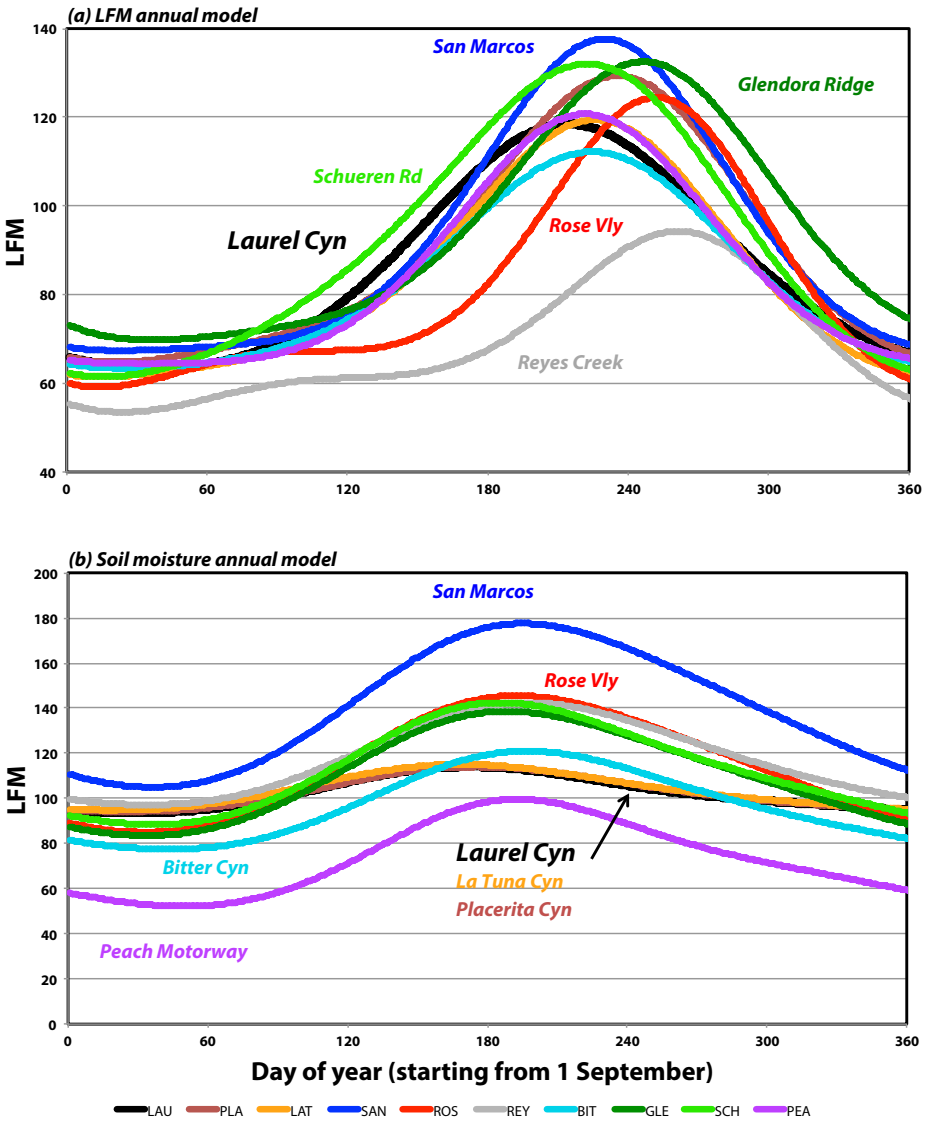

FIG. 3. (a) LFM annual models for ten sites selected for analysis, based on a day-of-year measure that for convenience starts on September 1^{st}; and (b) As in (a), but for the soil moisture annual model.

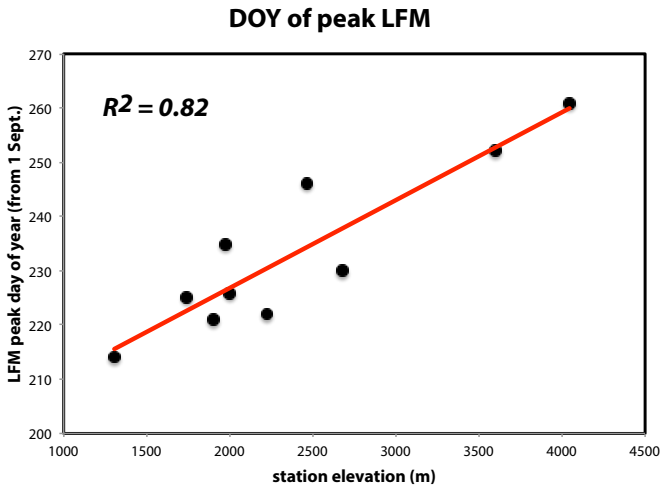

FIG. 4. Scatterplot of the LFM peak day-of-year (starts on September 1^{st}) vs. station elevation (m). The least squares fit is shown, with R^2=0.82.

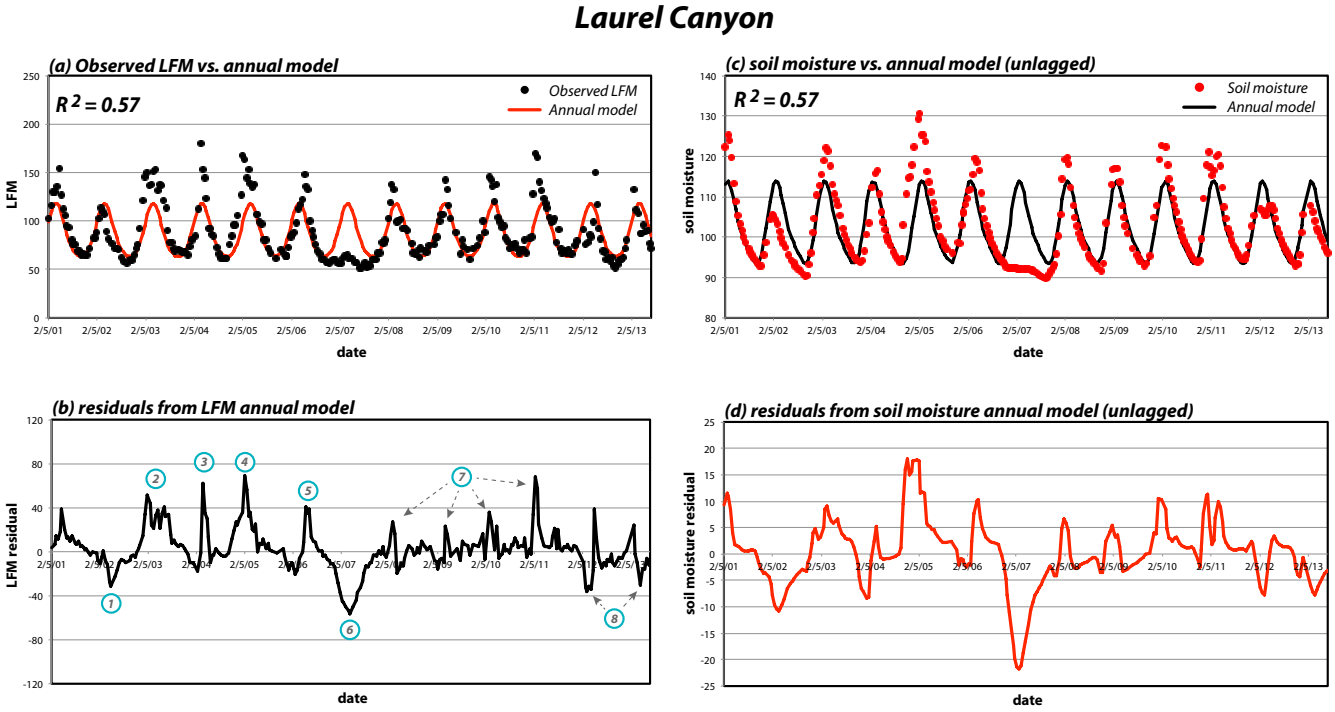

FIG. 5. Time series of (a) the observed LFM (black dots) vs. the annual model predictions (red curve), R^2=0.57; (b) the residuals from LFM annual model; (c) the soil moisture (red dots) vs. the unlagged annual model prediction(black curve), R^2=0.57; and (d) the residuals from the unlagged soil moisture annual model at Site Laurel Canyon. Circled numbers are special episodes referred in the text.

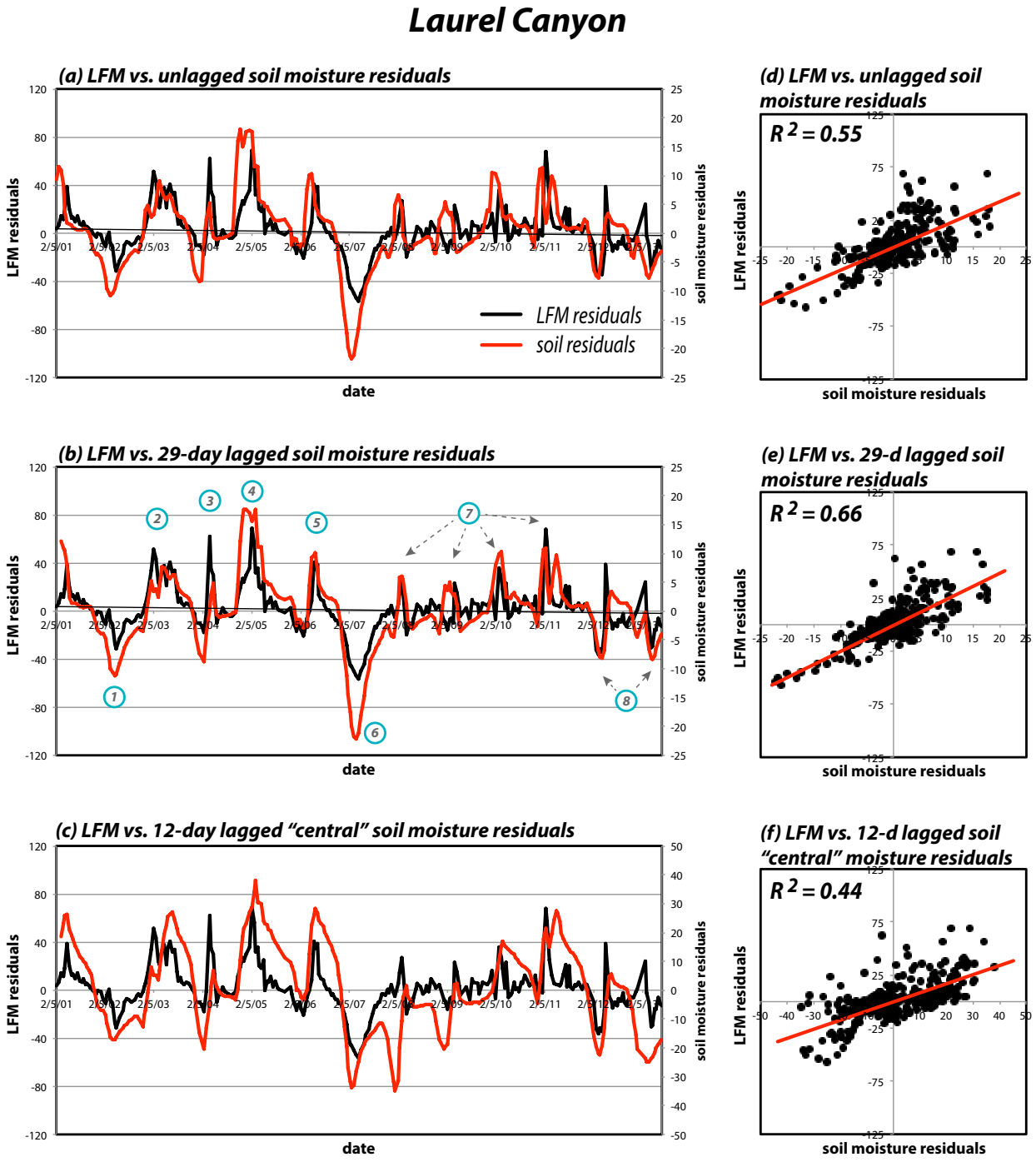

FIG. 6. Time series for the Laurel Canyon site of (a) the LFM residuals (black) vs. the unlagged soil moisture residuals (red); (b) the LFM vs. the 29-day lagged soil moisture residuals; and (c) the LFM vs. the 12-day lagged "shifted" soil moisture residuals; and (d-f) are the LFM scatterplots of the LFM residuals vs. the soil moisture residuals of (a-c), with the leas-squares fitting line overlaid, and R^2s being 0.55, 0.66 and 0.44 respectively. Circled numbers are special episodes referred in the text.

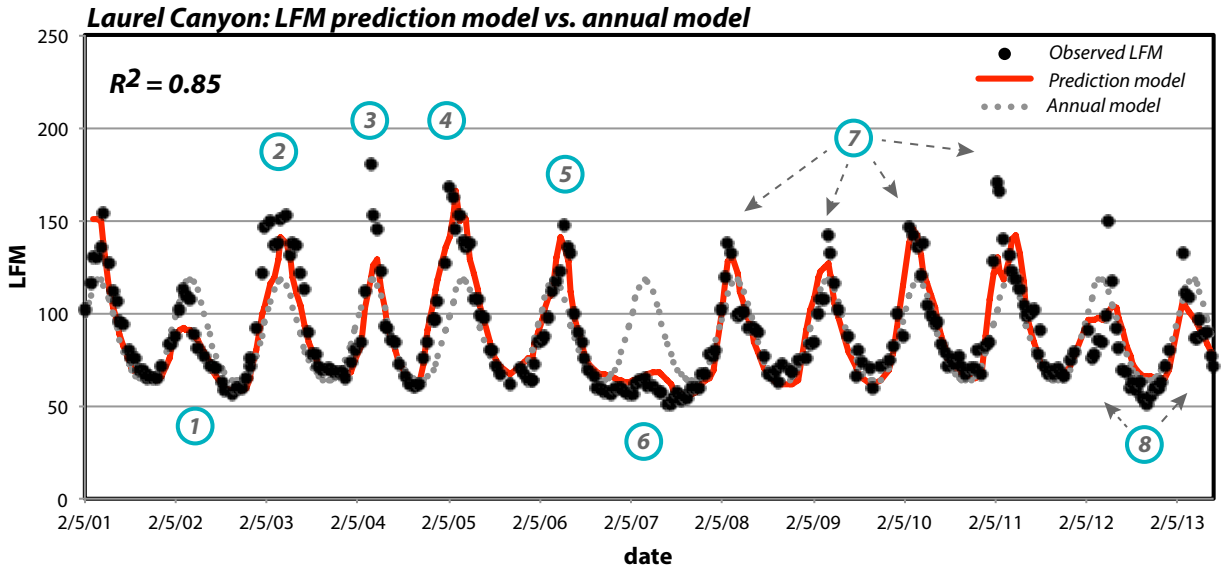

FIG. 7. The time series of the LFM prediction model (red curve) vs. the annual model (dotted line), with R^2 =0.85. Circled numbers are special episodes referred in the text.

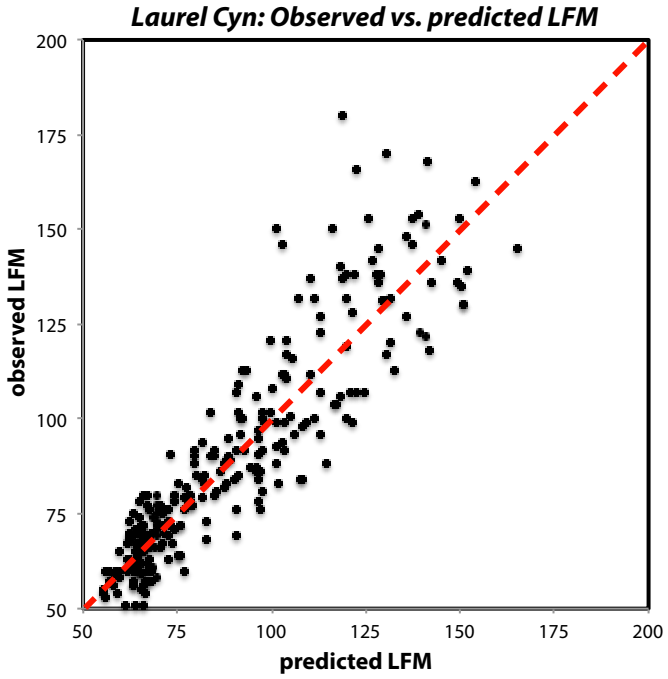

FIG. 8. Scatterplot of the observed LFM vs. the predicted LFM at site Laurel Canyon. Note that while LFM is shown here, the model was based on the natural logarithm of LFM.

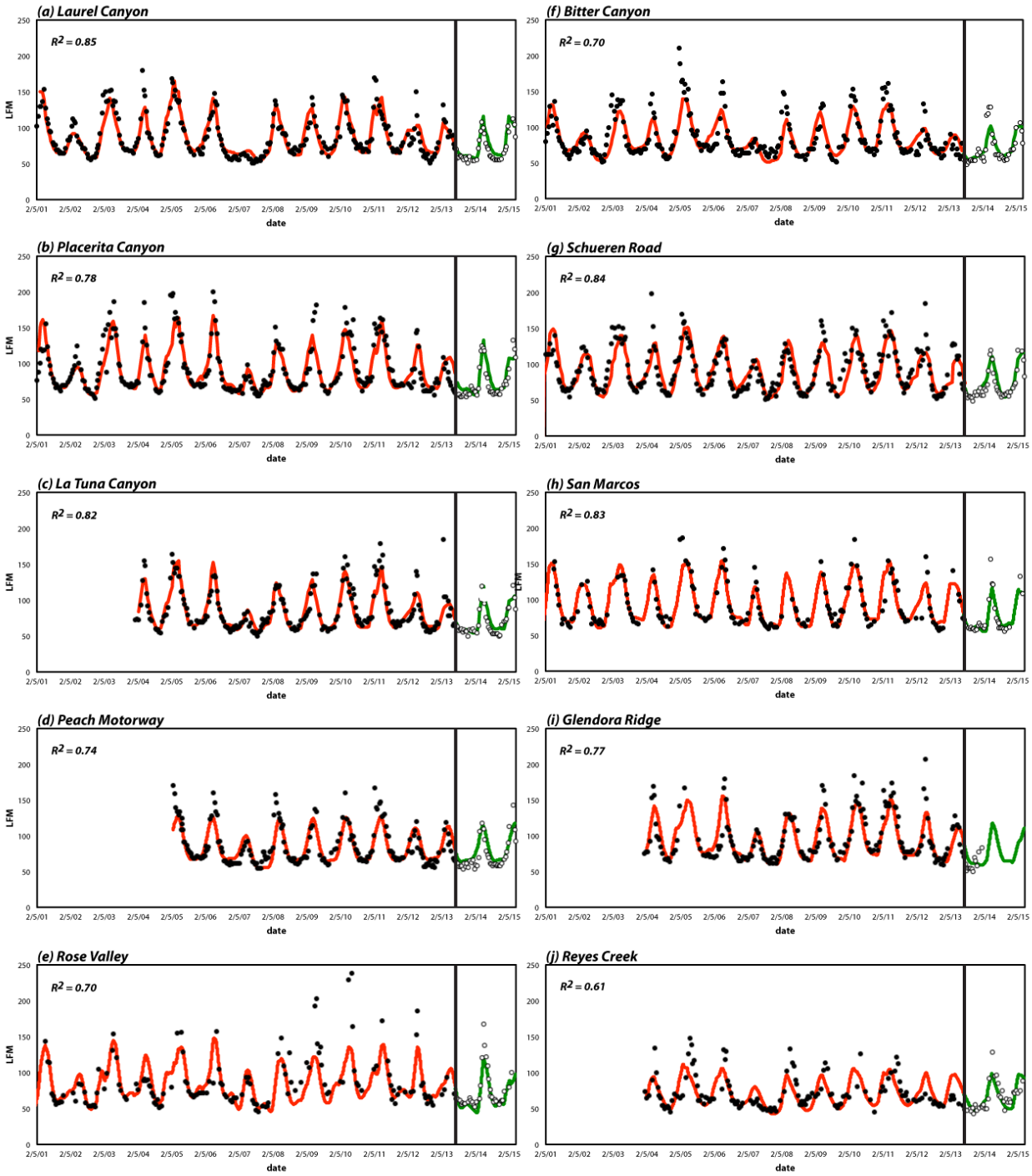

FIG. 9. Time series of the predicted (red curves) and the observed (black dots) LFM for stations (a) Laurel Canyon; (b) Placerita Canyon; (c) La Tuna Canyon; (d) Peach Motorway; (e) Rose Valley; (f) Bitter Canyon; (g) Schueren Road; (h) San Marcos; (i) Glendora Ridge, and (j) Reyes Creek. The (roughly two year) time period to the right of the thick vertical dashed line represents out-of-sample observations (white dots) and predictions (green curves). The model R^2s are based on observations to the left of the dashed lines. LFM observations were not available at Glendora Ridge after 10 January 2014.

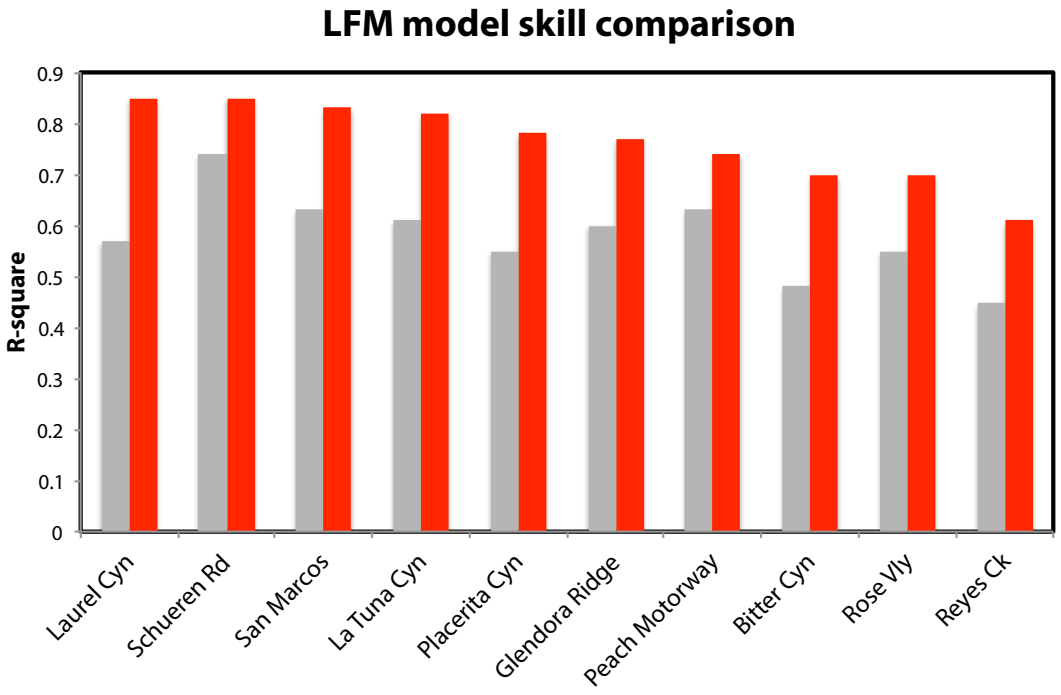

FIG. 10. Comparison of LFM explanatory skill for annual (TF) models (grey bars) and full prediction models (red bars).

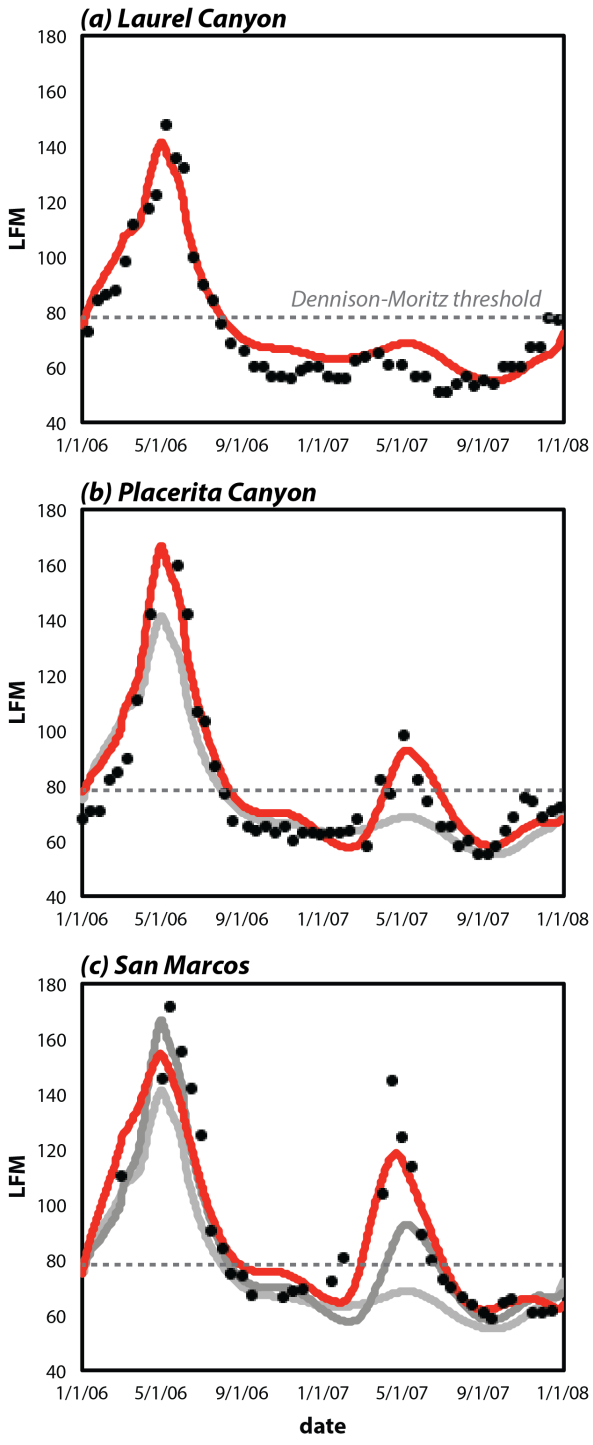

FIG. 11. Observed (black dots) and predicted (red curves) LFM between January 2006 and January 2008 for (a) Laurel Cyn; (b) Placerita Cyn; and (c) San Marcos. On panels (b) and (c), predictions from stations shown above also included for reference.

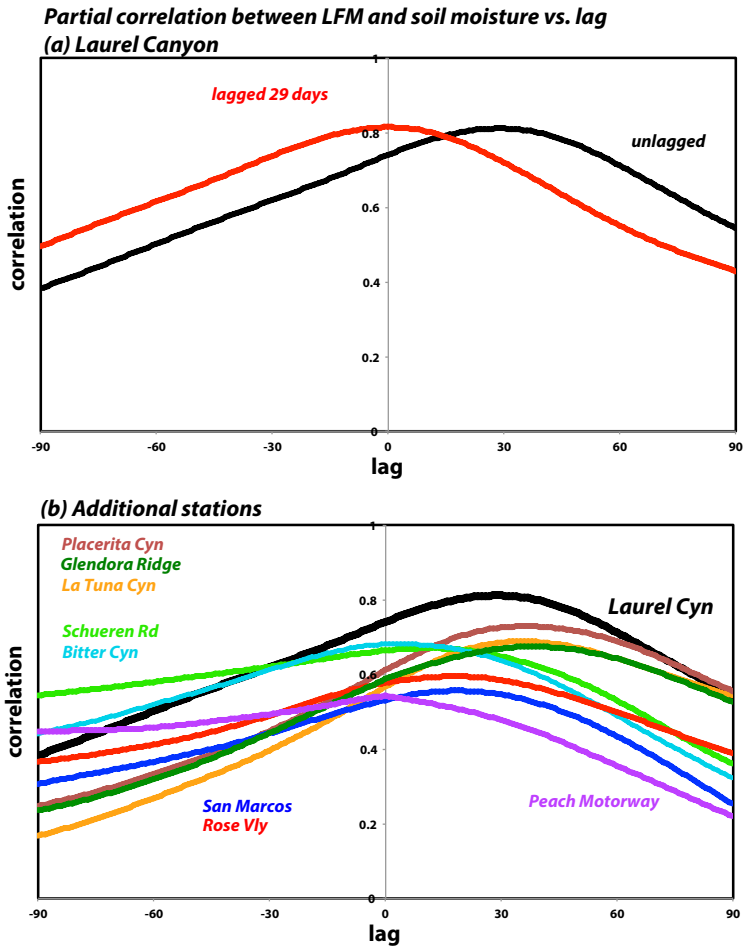

FIG. 12. (a) Partial correlation between LFM and soil moisture vs. the time lag applied to the soil moisture for site Laurel Canyon (black), including correlation curve after 29 day shift. (b) same as (a), but unshifted partial correlations for additional sites Placerita Canyon, Glendora Ridge, La Tuna Canyon, Schueren Road, Bitter Canyon, San Marcos, Rose Valley, and Peach Motorway.

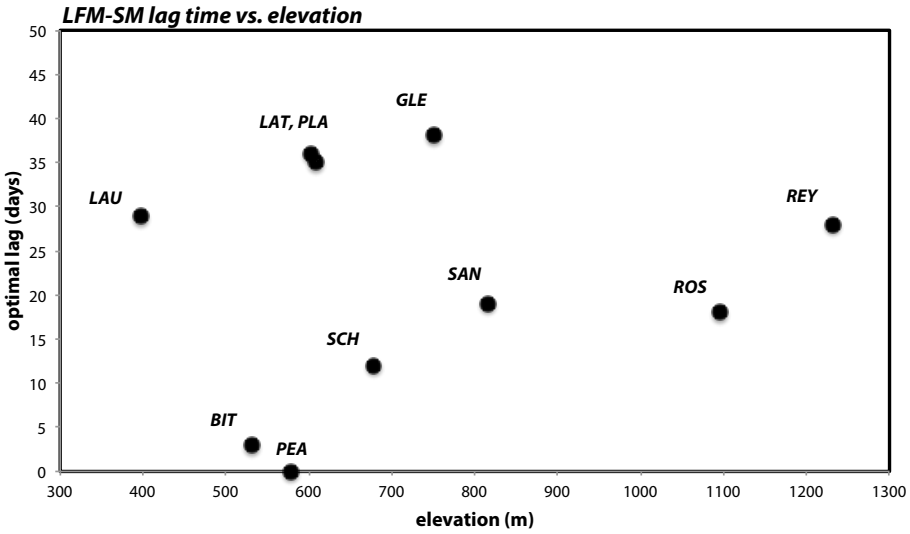

FIG. 13. The optimal LFM-soil moisture lag (days) vs. the site elevation (m).